



# The role of individual forcings in driving the wave-like recent trends in northern hemisphere summer atmospheric circulation.

Gerard Marçet-Carbonell<sup>1, 2</sup>, Markus G. Donat<sup>1, 3</sup>, and Carlos Delgado-Torres<sup>1</sup>

<sup>1</sup>Barcelona Supercomputing Center (BSC), Barcelona, Spain

<sup>2</sup>Facultat de Física, Universitat de Barcelona (UB), Barcelona, Spain

<sup>3</sup>Institució Catalana de Recerca i Estudis Avançats (ICREA), Barcelona, Spain

**Correspondence:** Gerard Marçet-Carbonell (gerard.marçet@bsc.es)

**Abstract.** The summer climate in the Northern Hemisphere during recent decades has shown distinct trend patterns, with warming hotspots that spatially match with the ridges of a circumpolar atmospheric wave-5 pattern in the upper troposphere. The drivers behind this wave-like trend and warming pattern are not yet well understood. Through the use of the Large Ensemble Single Forcing Model Intercomparison Project (LESFMIP) and the Atmospheric Model Intercomparison Project (AMIP) 5 simulations, we study the contributions of different forcing components as well as the role of oceanic temperature variability to the observed changes. Analysis of the single-forcing experiments shows that in particular historical anthropogenic aerosol forcing leads to responses that have some pattern similarity with the observed changes in atmospheric circulation, diagnosed from the 200 hPa geopotential height (Z200) after removing the zonal mean. However, despite high pattern agreement, the magnitude of the trends is underestimated in models. Our results suggest that the observed spatial structure of trends in Z200 10 is at least partially caused by anthropogenic aerosol emissions and is not the result of global warming caused by greenhouse gas emissions, and highlight important inconsistencies between models and observations.

## 1 Introduction

Anthropogenic global warming since pre-industrial times is now unequivocal (Intergovernmental Panel On Climate Change (Ipcc) (2023)), with associated increases in heatwaves and precipitation extremes (Robinson et al. (2021)). The observed trends, 15 however, are not spatially homogeneous and show pronounced regional variations (Lewis et al. (2017)), with evidence of these regional differences being related to changes in the atmospheric circulation (Vautard et al. (2023), Rousi et al. (2022), Horton et al. (2015)).

Understanding atmospheric circulation change is, therefore, important as it is a key driver of surface climate and is associated with regional weather conditions and extreme events. For instance, the "Dust Bowl", a devastating drought affecting the U.S., 20 Mexico and part of Canada in the 1930s, was linked to a change in the upper tropospheric circulation caused by anomalies in tropical sea-surface temperatures (SST) (Schubert et al. (2004)), and record high temperatures that lasted as records until the early 21st century were set during the Dust Bowl years in central parts of North America (Donat et al. (2016)). Increased hurricane activity in the Atlantic during 1995 to 2000 is linked to an increase in tropical Atlantic SST interacting with the



25 overlying tropospheric circulation that reduced vertical wind shear (Goldenberg et al. (2001)). Atmospheric circulation has also been identified as the primary influence of UK surface climate (Fereday and Knight (2023)).

Despite its importance as a driver of regional climate, atmospheric circulation is difficult to predict and is a major source of uncertainty in climate projections due to its chaotic nature and errors in modelling the circulation response to climate forcing (Shepherd (2014)). There is increasing evidence that shows how climate models appear to underestimate the atmospheric circulation changes in response to forcing. Some examples include the underestimation of summer temperatures and extremes 30 trends over Europe due to trends in southerly flow being underestimated in models (Vautard et al. (2023)), and the underestimation of the magnitude of North Atlantic Oscillation (NAO) variations in model ensembles due to the ratio of the predictable signal to unpredictable noise being too small in models (Smith et al., 2025)

35 The challenges to understand changes in atmospheric circulation are also highlighted in a recent study by Teng et al. (2022), where a non-homogeneous warming trend during 1979–2020 in the Northern Hemisphere (NH) boreal summer months (JJA) coinciding with a similar trend in 200 hPa geopotential height (Z200) is reported. The pattern observed in the trend resembles 40 that of a circumglobal wavenumber-5 Rossby wave. The observed warming differs from the more homogeneous warming projected at the time by CMIP5 models (Knutti and Sedláček (2013)), and the CMIP6 multi-model mean shows a more homogeneous trend in Z200 (Teng et al. (2022)). We currently do not have a clear understanding of what is driving these observed changes and why the CMIP6 ensemble mean is underestimating the magnitude of the regional variations of Z200 trends.

45 Knowing the causes behind the recent trends is key because it informs our anticipation of how these trends may evolve in the future, and can guide model developers in improving the representation of these processes. Current hypotheses centre around interdecadal modes of ocean variability such as the Atlantic Multidecadal Variability (AMV) (Trenberth and Shea (2006)) and Interdecadal Pacific Oscillation (IPO) (Henley et al. (2015)) contributing to the observed changes (Teng et al. (2022)). However, in recent years there has been new literature highlighting the role of aerosol and GHG emissions in shaping different 50 features of summertime Northern Hemisphere circulation such as storm-track weakening (Kang et al. (2024), Chemke and Coumou (2024)) and jet-stream weakening (Dong et al. (2022)). The effect of aerosols and other forcings such as GHGs, ozone or volcanic influence remaining unexplored in the context of the recent wave-like Z200 trends.

55 In this study, we aim to understand how different radiative forcings and observed ocean temperature variations affect trends in Z200 and to get a better understanding of the mechanisms responsible for the recent observed changes. To do so, we leverage simulations from the Large Ensemble Single Forcing Model Intercomparison Project (LESFMIP) (Smith et al. (2022)) and the Atmospheric Model Intercomparison Project (AMIP) (Eyring et al. (2016)).

## 2 Data and methods

To analyse atmospheric circulation patterns in the higher troposphere, we used monthly means of Z200 over the Northern 55 Hemisphere during the following two different periods: 1943–1978 and 1979–2014. 1979–2014 was chosen based on the previous literature (Teng et al. (2022)) and because historical simulations end in 2014. We decided not to concatenate the



historical runs with scenario simulations as these do not include observed forcings. The 1943–1978 period was chosen to complement the analysis of recent changes with a different period, and understand the evolution of the trend in time and identify possible differences in the mechanisms involved.

60 In the study we used three different reanalysis datasets to get estimates of the observed changes in atmospheric circulation: ERA5 (Hersbach et al. (2020)), NCEP-1 (Kanamitsu et al. (2002)) and JRA-3Q (Kosaka et al. (2024)). Given the similarities between their trends (Fig. S1) we used ERA5 as reference dataset, and show the respective analysis with JRA-3Q and NCEP-1 in the supplementary information (Fig. S4–S7). To disentangle the contributions that different forcings exert to the observed changes in atmospheric circulation, we used climate model simulations from LESFMIP (Smith et al. (2022)). LESFMIP produces simulations for different forcings, isolating each forcing at a time. More specifically, we used simulations isolating anthropogenic aerosol concentration, well-mixed GHG concentrations, volcanic emissions, solar activity changes, total ozone concentrations, as well as historical forcing simulations combining all of the above. To sample internal variability we selected models with at least 10 members per forcing configuration, so that the ensemble mean can be considered a reliable estimate of the model-specific forcing response. In total, 1687 simulations from 11 models (ACCESS-ESM1-5 (Ziehn et al., 2020),  
65 CanESM5 (Swart et al., 2019), CMCC-CM2-SR5 (Cherchi et al., 2019), E3SM-2-0 (Golaz et al., 2022), GISS-E2-1-G (Kelley et al., 2020), HadGEM3-GC31-LL (Andrews et al., 2020), IPSL-CM6A-LR (Boucher et al., 2020), MIROC6 (Tatebe et al., 2019), MPI-ESM1-2-LR (Gutjahr et al., 2019), MRI-ESM2-0 (Yukimoto et al., 2023), NorESM2-LM (Seland et al., 2020))  
70 were used. Different parametrizations of a given model were treated as different models. We indicated this by adding the label p+number of parametrizations to models with parametrizations different from p1. A complete list of all the models and members  
75 used can be found in Table S1.

To quantify the potential effect of SST forcing, we also analysed Atmospheric Model Intercomparison Project (AMIP) simulations (Eyring et al. (2016)). These are idealized atmosphere-only experiments that use SSTs and sea ice concentration from reanalysis data as boundary conditions as well as prescribed historical forcings. While not being a coupled system, therefore missing feedback mechanisms between ocean and atmosphere, these simulations represent ocean variability patterns  
80 and modes in sync with the observed climate. Given the current hypothesis centred around ocean variability driving the recent trends (Teng et al. (2022)), we used AMIP simulations to assess if representation of observed SST variations leads to better representation of trends in geopotential height (GPH). Only models with at least three members have been selected to be able to filter out internal variability, which provides a total of 60 simulations from nine models (ACCESS-ESM1-5 (Ziehn et al., 2020), CanESM5 (Swart et al., 2019), E3SM-2-0 (Golaz et al., 2022), GISS-E2-1-G (Kelley et al., 2020), HadGEM3-GC31-  
85 LL (Andrews et al., 2020), IPSL-CM6A-LR (Boucher et al., 2020), MIROC6 (Tatebe et al., 2019), MPI-ESM1-2-LR (Gutjahr et al., 2019), MRI-ESM2-0 (Yukimoto et al., 2023)) for the analysis. A list with the AMIP models and members used can be found in Table S2.

To remove the thermal expansion imprint on Z200, we removed the zonal mean of geopotential height at each latitude and summer season. We will refer to this new variable as the azonal component of Z200, i.e. Z200\_az. We then computed the linear  
90 trend for each of the periods (1943–1978 and 1979–2014) of Z200\_az in:

- Reanalysis.



- Each individual member of both LESFMIP and AMIP simulations.
- The model specific ensemble mean for each forcing and model of LESFMIP and AMIP.
- The multi-model ensemble mean for each forcing and AMIP.

95 The model specific ensemble means were obtained by taking the mean at each point in space and time of all members of the corresponding forcing and model. The multi-model mean was computed averaging all respective model-specific ensemble means, thus all models contribute equally regardless of their ensemble size. The linear trends in atmospheric circulation were computed by means of a least squares linear regression, and the statistical significance of the trends was assessed using a two-sided t-test at the 95 % confidence level. We accounted for autocorrelation in the data by applying an effective sample  
100 size correction assuming a first order autocorrelation of the data residuals (Wilks, 2011). Similarity of the spatial patterns of changes between models and reanalysis was assessed using the area-weighted Pearson pattern correlation at midlatitudes (30° N-60° N) for the whole circumference and the two longitude ranges defined in Happé et al. (2025): Eurasia (15° E - 110° E) and North America - Atlantic (NA-Atl) (100° W - 0° E). Significance of the pattern similarity was assessed using block  
105 bootstrap resampling at the 95 % confidence level. All reanalysis and model simulations were interpolated by means of bilinear interpolation to a common 2.5°x2.5° grid.

### 3 Results

#### 3.1 Forced responses

The 1979–2014 trends in Z200\_az in NH summer present a clear circumglobal wave-5-like pattern as was documented in depth in Teng et al. (2022) (Fig. 1a). The different multi-model ensemble means, on the other hand, present a wide range  
110 of trends (in both magnitude and spatial distribution of changes) for the same period depending on the forcing configuration of each multi-model ensemble (Fig. 1). Our results indicate that only simulations forced with anthropogenic aerosol or well-mixed greenhouse gas emissions show significant trends in NH midlatitudes Z200\_az during summer (Fig. 1b–i). This suggests that natural radiative forcings (solar and volcanic) as well as ozone do not drive significant changes in Z200\_az in the model simulations, and do not play a role in driving the observed changes.

115 Regarding the spatial structure of the trends, the aerosol, AMIP and historical ensembles present very similar patterns (Fig. 1b–d). This indicates that the historical simulations are dominated by the aerosol response. Notable features are the decrease in Z200\_az in the North Atlantic, as well as the wave train over Eurasia with two centres of increased Z200\_az over central Europe and Asia combined with a decrease in Z200\_az between them over western Asia. This structure is present and significant in  
120 reanalysis (Fig. 1a). AMIP fails to capture the GPH increase over western Europe but captures better the quadrupole structure over the Pacific (Fig. 1c). The decrease in Z200\_az over west Asia is displaced Southward in the aerosol only experiments (Fig. 1d). Simulations forced with only well-mixed greenhouse gases (Fig. 1e), while showing some regionally significant trends, do not show a spatial structure of changes similar to reanalysis.

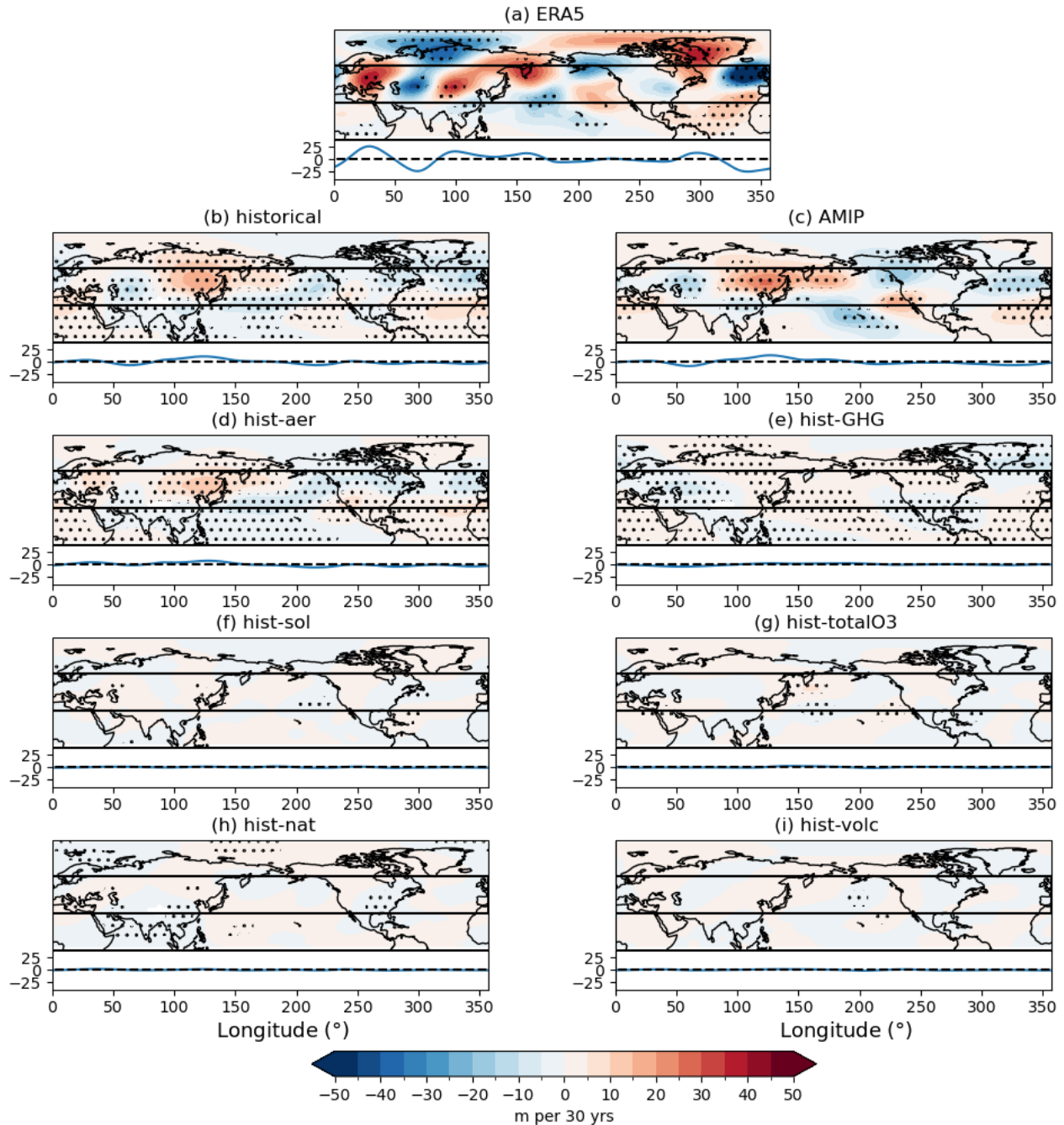


**Figure 1.** Trends of  $Z_{200\text{az}}$  [m per 30 yr] for the period 1979–2014 obtained with the ERA5 reanalysis (a) and the multi-model ensemble mean for each respective forcing (b–i). The line plot under each map represents the meridionally averaged trend from  $30^\circ\text{N}$  to  $60^\circ\text{N}$  (region enclosed by a black box in the maps). Stippling indicates statistically significant trends using a two-sided t-test at 95% confidence level.

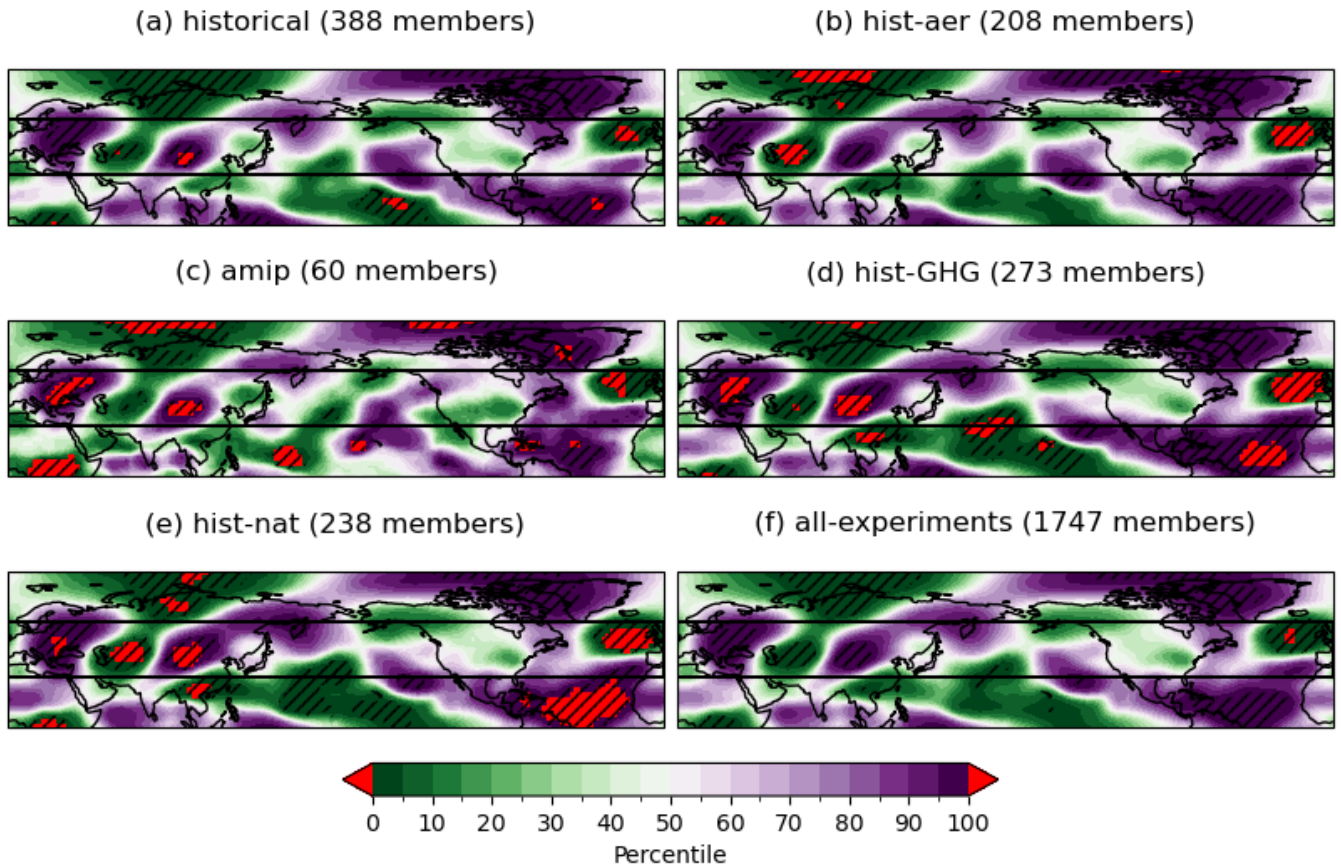


**Figure 2.** Percentile of ERA5 Z200\_az trends with respect to the trends in the individual simulations of specific forcing configurations (a–e) and all experiments combined (f). Hatching indicates where ERA5 lies below the 2.5th percentile or above the 97.5th percentile of simulated trends, and the red areas indicate that ERA5 is outside all model values.

The amplitude of the Z200\_az trends in those forcing configurations that present significant trends (AMIP, historical, aerosols and GHG) is in all cases appreciatively fainter than that of the reanalysis. Out of the 4 forcing configurations, AMIP shows the 125 largest amplitude. However, AMIP has fewer ensemble members per model than each LESFMIP forcing experiment (Tables S1 and S2). The amplitude of the trends in reanalysis is not only stronger than that of the ensemble means, but often also than that of individual members. As can be seen in Fig. 2, all the main hotspots over Eurasia fall outside of the model range of trends for natural and GHG forcings (Fig. 2d, e). Some of them fall outside the range of trends in the historical, aerosol or AMIP simulations (Fig. 2a–c). This is the case despite the large ensemble sizes (60 for AMIP, between 208 and 388 for LESFMIP), 130 indicating that there is a systematic underestimation of changes in Z200\_az in models in these regions where the observed trends are strongest. Even taking into account all 1747 simulations from combining all experiments, reanalysis falls outside all model trends in regions of the North Atlantic (Fig. 2e) consistent with the findings in D'Andrea et al. (2024).

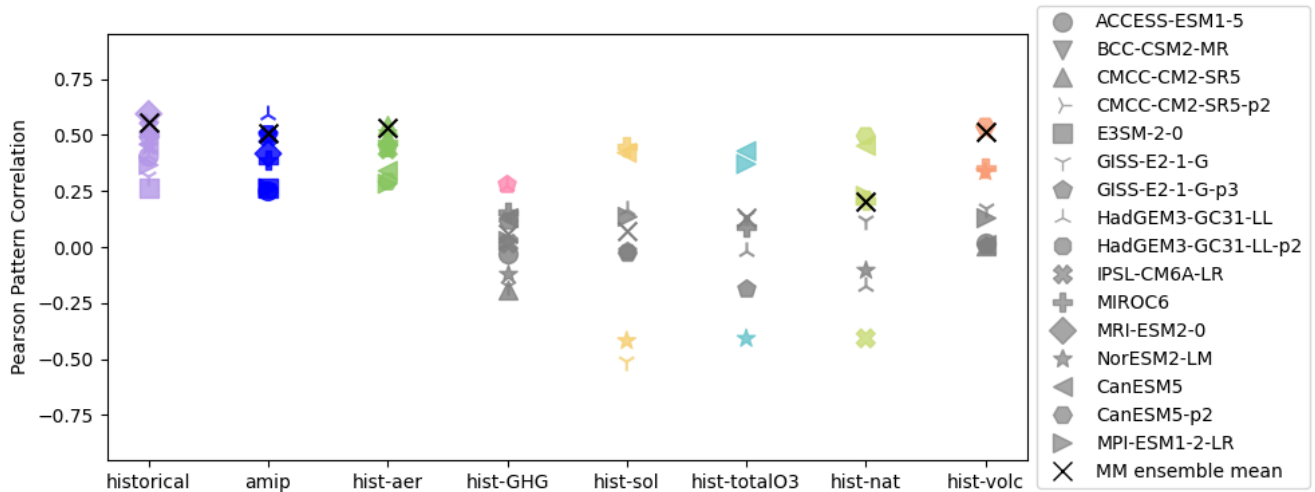


**Figure 3.** Pearson pattern correlation of model-specific ensemble averages of the Z200\_az trend with respect to ERA5 during 1979–2014. Each different model mean is represented by a different shape. Multi-model ensemble means for each forcing are shown with a black cross. Non-significant correlation values are shown in grey.

We next quantify the similarities in spatial patterns of the trends between the different model ensembles and reanalysis through Pearson pattern correlation. As we can see in Fig. 3 for 1979–2014, AMIP simulations and experiments using aerosol and historical forcings show similar values of positive pattern correlation across all models, while GHG consistently show correlation values around zero with reanalysis. This indicates that the historical forcings, and in particular aerosol forcing, have at least a partial effect in driving the trends in Z200\_az. Whereas changes stemming from GHG forcings do not correlate to the trends in reanalysis. Therefore, these results suggest that GHG emissions alone, and the associated global warming, do not play a role in driving the observed trends in Z200\_az. The similarity in pattern correlation between AMIP and historical simulations implies that realistic representation of modes of ocean variability in models is not related to an increase in pattern similarity over what the historical forcing simulations show. Accordingly, we find no evidence for oceanic variability contributing to the wave-5 like trend pattern in Z200\_az. However, while not appreciated using this metric, AMIP simulations show better representation of Z200\_az changes over the Pacific compared to historical simulations (Fig. 1b,c).

If instead of studying the whole midlatitudes we focus on Eurasia and NA-Atl longitudes (similar to Happé et al. (2025)) the results become more noisy as the region studied is smaller. Accordingly, for the NA-Atl region (Fig. 4a) the pattern correlation values for aerosols and GHG become comparable, with larger variations and less significant values in the aerosol simulations compared to the whole circumference. On the other hand, the Eurasia region (Fig. 4b) shows higher pattern correlation and results consistent with the whole circumference. Therefore, different regions of the circumglobal wave-5 pattern may have different drivers as was also shown for shorter term variability by Happé et al. (2025). Additionally, despite high correlation values in some cases, none of the multi-model ensemble means captures the increase in geopotential height over Greenland

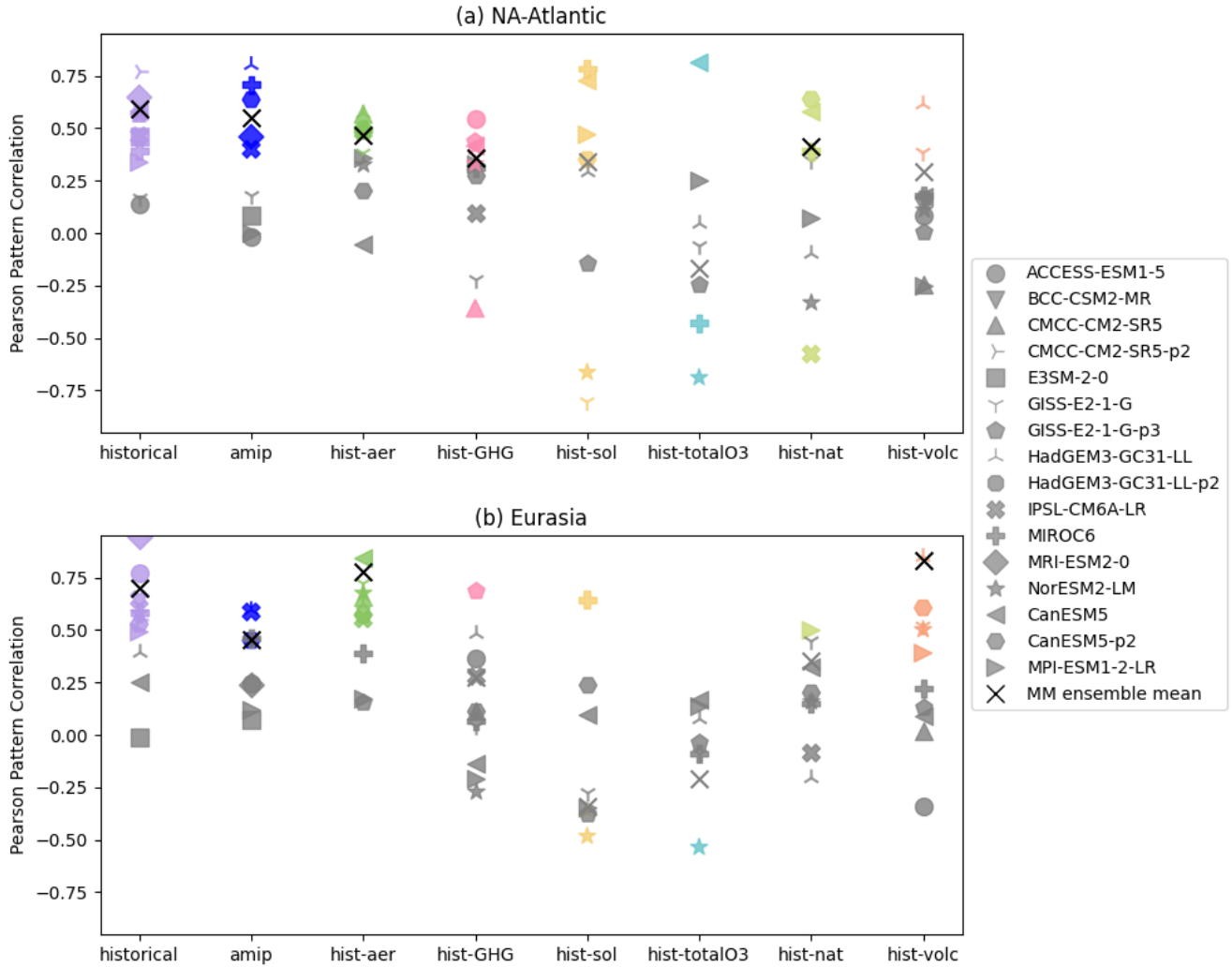


**Figure 4.** As Fig. 3 but for the NA-Atl region (a) and Eurasia (b).

associated with the wave pattern over the NA-Atl region in line with the reported model error in reproducing Greenland Blocking (GB) trends (Maddison et al. (2024), Hanna et al. (2018))

### 3.2 Variability in individual simulations

In addition to the trends of the ensemble mean (representative of the forced response), we explore the range of trends in the 155 individual simulations for each forcing experiment. All forcing configurations during 1979–2014 have a large spread in pattern correlations across the individual ensemble members, with several members presenting negative correlation values (Fig. 5). This includes AMIP simulations, indicating that prescribed SSTs are not enough to constrain the atmospheric circulation

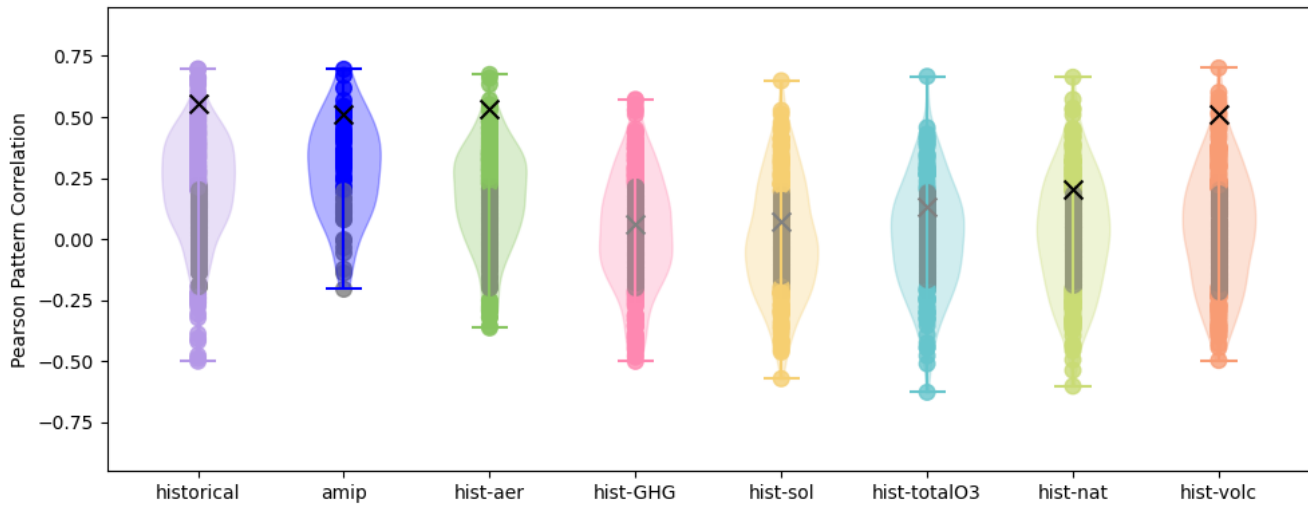


**Figure 5.** Pearson pattern correlation of the Z200\_az trends in the individual simulations with respect to ERA5 during 1979–2014. Violin plots represent the probability density function estimated by a Gaussian kernel density estimator. Multi-model means for each forcing are shown with a black cross. Non-significant correlation values are shown in grey.

trends. Out of all the forcing configurations only AMIP, historical and aerosol forced runs show distributions skewed towards positive values of pattern correlation.

160 The differences between different members of the same model are, by design, reflecting uncertainty from internal climate variability in the models. This suggests that, in the model simulations, internal variability is a strong contributor to the trend patterns. If internal variability in the models is representative of internal variability in the real world, there would be a strong contribution of internal variability to the observed circulation changes. However, as the AMIP experiments do not show enhanced pattern similarity compared to the historical or aerosol forcing simulations, we cannot associate this internal variability 165 with large-scale modes of ocean variability.

In Fig. 6 we show that there is a large overlap between distributions of pattern correlations across different models, indicating that the large spread does not arise from different model behaviours. And models that provide a larger ensemble size tend to have a larger spread across their ensemble members. It can also be appreciated how model mean trends are in the higher end of the distribution for aerosol, AMIP and historical, reinforcing the idea that the observed trends are in part a response to forcing. 170 As the forced response derived from averaging different members tends to be more similar to the observed trends than the average individual member.

### 3.3 1943–1978 period

To complement the analysis of changes in the northern hemisphere summer atmospheric circulation during the most recent decades, we also analyse the observed and modelled changes in an earlier period. During 1943–1978, the trend pattern in Z200

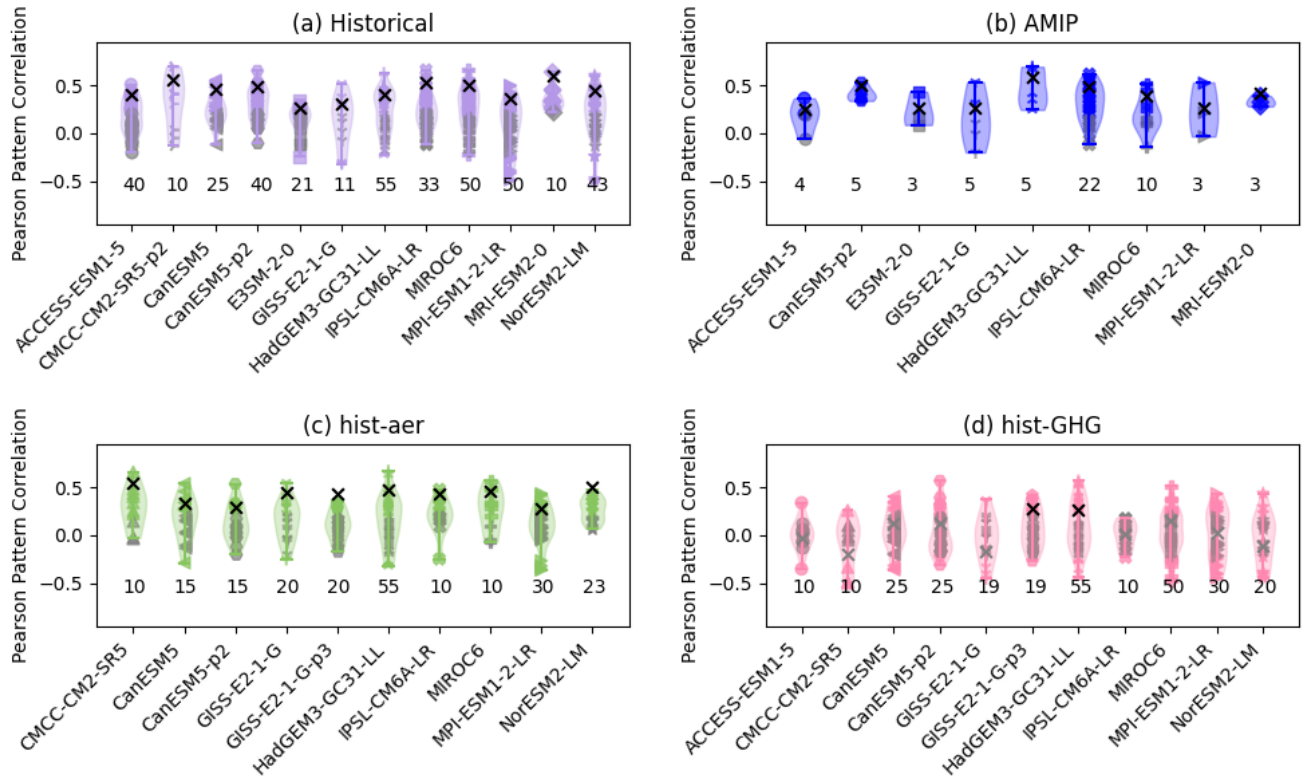


**Figure 6.** Pearson pattern correlation of the trends in Z200\_az in each individual simulation for different forcing experiments with the trends in ERA5: historical (a), AMIP (b), aerosols (c) and GHG emissions (d). Non-significant correlation values are shown in grey. Violin plots represent the probability density function estimated by a Gaussian kernel density estimator. Pattern correlation of the trend of model means are shown with a black cross (these correspond to the values shown in Figure 3). The numbers above the x-axis indicate the number of members per model in each forcing experiment.

175 is largely different to that of 1979–2014 in reanalysis, with opposite changes in some regions between the two periods (Fig. S2a). This indicates that the changes in GPH are time dependent, with a reversal of the trends between the two periods in some regions (compare Fig. 1a and Fig. S2a). When analysing the pattern similarity of the different model experiments with the reanalysis trends, we get, however, similar results as for the more recent period: Also for the earlier period, aerosol forcing dominates the historical forcing response. Both historical and aerosol simulations reproduce some of the more prominent 180 features in reanalysis, such as the decrease in GPH over northeast Asia, at a much fainter magnitude than in the reanalysis (Fig. S2b,c). Note that the AMIP simulations are not available for this earlier period, and so cannot be included in this analysis. In this earlier time period, the GHG simulations do not show significant trends (Fig. S2d).

Also for this earlier time period, and similar to our findings for the more recent trends discussed above, the pattern correlations of the ensemble means and reanalysis show similar values between historical and aerosol-only simulations (Fig. 7). These

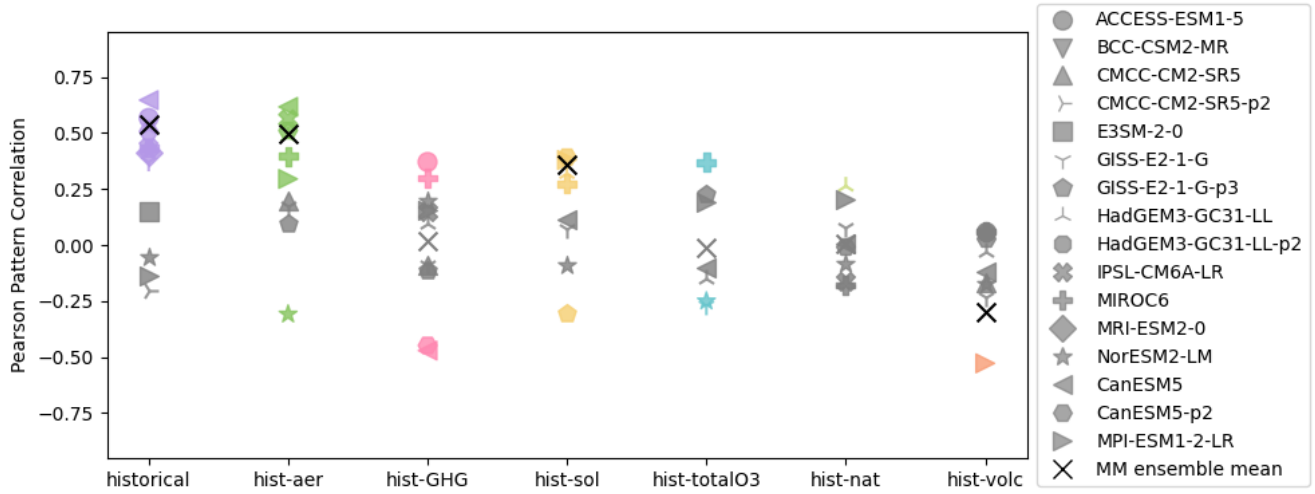


**Figure 7.** As Fig. 3, but for 1943–1978. AMIP simulations are not available for this period.

185 model-specific pattern correlation values, however, present a larger spread than in the 1979–2014 period (compare Fig. 7 and Fig. 3). These results suggest that aerosol emissions contributed, at least partially, also to the observed changes in Z200\_az during 1943–1978, and based on the LESFMIP experiments we find no evidence that GHGs and natural radiative forcings were driving the observed changes in Z200\_az. Finally, individual simulations present a large spread in pattern correlations (Fig. S3), as was the case during the later period (Fig. 5), indicating that internal variability plays a strong role in the simulated 190 changes also for that earlier time period.

#### 4 Discussion

Our results show that to some extent the model simulations that include aerosol forcing, were able to capture the spatial patterns 195 of the observed atmospheric circulation changes on the northern hemisphere during summer during the last decades, showing multi-decadal trends similar to a wave-5 pattern (as defined in Teng et al. (2022)). This, together with the appreciatively different response of models to different forcings is indication that the observed trends have a forced component. Similarly, the lack of significant trends in volcanic, solar and ozone concentration forcing configurations points towards these forcings not meaningfully affecting the spatial structure of Z200 during the analysis period.

Similarly, GHG emissions-only forced simulations did not show significant trends in Z200\_az during 1943–1978 and showed 200 no agreement in pattern correlation to reanalysis during 1979–2014. This suggests that global warming related to enhanced GHG emissions alone has not contributed to the spatial structure of trends in northern hemisphere atmospheric circulation during summer, as measured by Z200\_az, in recent decades.



The magnitude of trends in the simulations, on the other hand, is appreciatively smaller than in the reanalysis for all forcing configurations. This is the case for both ensemble means (indicating the model-specific responses to forcing) and, to a lesser extent, also in individual simulations. The smaller magnitude of trends in the ensemble means implies that the forcing response 205 is small based on the models that we used. This means that either other processes than radiative forcings are driving the largest part of the observed changes (e.g. internal variability), or that the models are underestimating the forced response. This latter possibility is consistent with the documented signal-to-noise problem in climate models, which indicates that model simulations underestimate the strength of the predictable signal (Scaife and Smith, 2018) and responses to forcings (Smith et al., 2025). On the other hand, the smaller magnitude of changes in individual simulations highlights that even considering the forcing 210 response together with internal variability, models are not capturing the magnitude of the observed trends in some regions. If the observed trend is linked to extreme events at the surface as proposed in Teng et al. (2022), underestimation of changes of atmospheric circulation in models could hinder our ability to predict these events.

Notably, aerosol-only forced runs are able to match to a large degree the changes in Z200\_az from historically forced runs and to a lesser extent reanalysis data. This points to aerosols being an important contributor to the trends in Z200\_az during summer. 215 However, there are some patterns that are not well captured in the models. More specifically, the increase in geopotential height over Greenland is not present in any of the multi-model ensemble means (Fig. 1). This increase in geopotential height over Greenland has been related to an increase in GB events linked to SST and aerosol forcing, underestimated in models (Maddison et al. (2024), Hanna et al. (2018)). This finding would be consistent with the multi-model ensemble means not showing a clear increase in Z200\_az over Greenland.

220 At the same time, without clear understanding of the physical mechanisms behind the changes it is challenging to attribute the different regional behaviours in models to model error or a faithful representation of disconnected wave patterns. The concrete mechanisms behind the changes are, however, not clear at this point. Aerosols, compared to GHG forcings, have a much more localized influence and present regional changes in effective radiative forcing during recent decades (Fiedler et al. (2023); Hoesly et al. (2018)).

225 Based on this, a possible explanation for the observed changes is a positive feedback between surface warming and Z200. The localized radiative effect of aerosols can generate localized heating in the surface, expanding the air and increasing the GPH in the column. This in turn could generate a high-pressure system which increases clear-sky conditions and warming through subsidence in turn driving change in the patterns of atmospheric circulation. This hypothesis is coherent with a recent study documenting a westward shift of heatwave hotspots linked to increased soil moisture-atmosphere coupling (Zhang et al. 230 (2025)), which could be accentuated by an increase in surface downward shortwave radiation net flux related to reductions in aerosol emissions over the mid-latitudes.

The effect of aerosol radiative forcing has also been linked to changes in the jet stream due to its repercussions on the meridional temperature gradient (Dong et al. (2022)). Therefore, an alternative possible mechanism of influence between aerosols and the Z200 trends could be via modulation of the Circumglobal Teleconnection (CGT) (Ding and Wang (2005)). 235 The CGT is defined as the 2nd principal component of Z200 during summer and takes the shape of a stationary Rossby wave embedded in the westerly Jet Stream (Ding and Wang, 2005). In recent decades the CGT structure has reportedly changed



(Tang et al., 2025). The observed changes in the CGT bear a large degree of similarity to the reported trend in Z200 and are facilitated by changes in the structure of El Niño Southern Oscillation and the westerly jet (Tang et al., 2025). Given that the changes in the westerly jet could be a result of aerosol radiative forcing (Dong et al., 2022), the observed trends in Z200 during 240 summer could therefore be a reflection of changes in the CGT linked to the effect of aerosols on the westerly jet.

Previous literature (Teng et al. (2022)) pointed at modes of ocean variability, in particular AMV and IPO, as possible drivers behind the observed changes in atmospheric circulation. In our study we did not find enhanced pattern similarity in AMIP compared to historical simulations. This, together with a large spread in individual AMIP runs, does not allow us to establish a clear link between boundary forcing from SSTs and the observed wave-5 trend. In contrast, Teng et al. (2022) did find 245 higher pattern correlation between the AMIP multi-model mean and reanalysis anomalies in Z200\_az compared to the CMIP6 multi-model ensemble, suggesting that the pattern similarity between model ensembles and reanalysis is sensitive to the way the ensemble is constructed. Concerning the magnitude of the model trends, the AMIP multi-model ensemble mean shows slightly higher magnitude compared to historical simulations and better pattern representation over the Pacific Ocean (Fig. 1b, c), but the much smaller ensemble size (60 members in AMIP and 388 members in historical) makes it difficult to draw a clear 250 conclusion.

Recent work (Happé et al. (2025)) highlights that there is an SST imprint preceding observed Rossby wave events which is not present in CMIP6 models, which could mean key feedbacks between SSTs and high troposphere atmospheric circulation are missing in these models, possibly explaining the lack of added similarity in AMIP runs if the changes are caused by ocean variability.

## 255 5 Summary and conclusions

In recent decades significant trends in Z200\_az on the NH during summer have been observed. However, there is not a clear 260 understanding of what has been driving these changes. In this study, we have used LESFMIP and AMIP simulations to study the contributions from the different radiative forcings and observed ocean temperature variations. More specifically, we quantified the degree of pattern similarity between the model simulations and observations with the aim of identifying which drivers play a role in shaping Z200 spatial trend patterns.

Our results suggest that aerosols played an important role in producing the observed changes, especially over the Eurasian region, presenting a spatial structure of changes very similar to that of historical simulations. GHG-only simulations, on the contrary, have little to no spatial correlation to the observed changes, suggesting that GHG-forced global warming did not drive the wave-5 like trends in the northern hemisphere summer atmospheric circulation. We did not find evidence for a link 265 between modes of ocean variability and the atmospheric circulation trends, as AMIP simulations had a similar degree of pattern similarity compared to historical and aerosol simulations.

Trends in the model simulations have a smaller magnitude than in the reanalysis. This is the case for ensemble means and to a lesser degree individual runs, with reanalysis trends falling outside the model response at the reported hotspots. We believe the low magnitudes in the ensemble means are indicative of a small forced response in models, likely related to signal-to-noise



270 issues in climate models (Scaife and Smith (2018)). While for individual simulations it indicates that some of the observed changes fall outside the range of simulated changes even when accounting for the internal variability of the models.

Follow-up research should explore the specific physical mechanisms by which aerosol emissions are driving the changes in summer atmospheric circulation, and understand the small signals of the forcing response. If these small signals are indications of so-called signal-to-noise errors, then it may be possible to develop calibrations aimed at correcting these errors (Smith et al. 275 2025). This may imply that in reality a larger part of the observed changes are happening in response to forcing than the small magnitude of the responses when taking the models at face value.

Finally, our finding that GHG-related warming is likely not a contributor to the observed wave-5-like atmospheric circulation changes, indicates that these changes may not continue as such under continued global warming in the coming decades. Depending on future aerosol emissions, some of these changes in atmospheric circulation and the associated accelerated warming 280 in some regions could even revert in the future. Accurate predictions will require better understanding of the specific processes, potential signal-to-noise errors, and regularly updated estimates of future aerosol emissions.

*Data availability.* The LESFMIP and AMIP data that is used in this work can be downloaded from the ESGF portal <https://esgf-ui.ceda.ac.uk/cog/search/cmip6-ceda/>. The ERA5 reanalysis can be downloaded from the Copernicus Data Store <https://cds.climate.copernicus.eu/datasets/reanalysis-era5-pressure-levels-monthly-means>. The JRA-3Q reanalysis can be downloaded from the Geoscience Data Exchange 285 portal [https://gdex.ucar.edu/datasets/d640002/](https://gdex.ucar.edu/datasets/d640002). The NCEP-1 reanalysis can be downloaded from the NOAA website <https://psl.noaa.gov/data/gridded/data.ncep.reanalysis.html>

*Author contributions.* GMC and MGD conceived the study, GMC performed the data analysis and wrote the first draft of the paper. All authors discussed the results and revised the text.

*Competing interests.* The authors declare that they have no conflict of interest.

290 *Acknowledgements.* We would like to acknowledge Tamara Happé, Rikke Stoffels, Dim Coumou, Jonathon Wright, Vincent Verjans, Pep Cos, Marta Brotóns, Alba Santos-Espeso and Michele Filippucci for the exchanges that helped shape this work. We would also like to thank Jonathon Wright, Shoshiro Minobe, David Avisar and Chaim Garfinkel for the LESFMIP data download in JASMIN and Margarida Samsó for the AMIP and reanalysis data download. This work used JASMIN, the UK's collaborative data analysis environment (<https://www.jasmin.ac.uk> Lawrence et al. (2013)). This study was funded by the European Union Horizon Europe research and innovation programme 295 under Grant Agreement 101137656 (EXPECT project) and by the predoctoral program AGAUR-FI ajuts (2025 FI-3 00065) Joan Oró, of the Department of Research and Universities of the Generalitat of Catalonia, as well as the European Social Plus Fund.



## References

Andrews, M. B., Ridley, J. K., Wood, R. A., Andrews, T., Blockley, E. W., Booth, B., Burke, E., Dittus, A. J., Florek, P., Gray, L. J., Haddad, S., Hardiman, S. C., Hermanson, L., Hodson, D., Hogan, E., Jones, G. S., Knight, J. R., Kuhlbrodt, T., Mios, S., Mizielski, M. S., Ringer, M. A., Robson, J., and Sutton, R. T.: Historical Simulations With HadGEM3-GC3.1 for CMIP6, *Journal of Advances in Modeling Earth Systems*, 12, e2019MS001995, <https://doi.org/10.1029/2019MS001995>, *\_eprint*: <https://agupubs.onlinelibrary.wiley.com/doi/pdf/10.1029/2019MS001995>, 2020.

Boucher, O., Servonnat, J., Albright, A. L., Aumont, O., Balkanski, Y., Bastrikov, V., Bekki, S., Bonnet, R., Bony, S., Bopp, L., Braconnot, P., Brockmann, P., Cadule, P., Caubel, A., Cheruy, F., Codron, F., Cozic, A., Cugnet, D., D'Andrea, F., Davini, P., De Lavergne, C., Denvil, S., Deshayes, J., Devilliers, M., Ducharne, A., Dufresne, J., Dupont, E., Éthé, C., Fairhead, L., Falletti, L., Flavoni, S., Foujols, M., Gardoll, S., Gastineau, G., Ghattas, J., Grandpeix, J., Guenet, B., Guez, E., L., Guilyardi, E., Guimbertea, M., Hauglustaine, D., Hourdin, F., Idelkadi, A., Joussaume, S., Kageyama, M., Khodri, M., Krinner, G., Lebas, N., Levavasseur, G., Lévy, C., Li, L., Lott, F., Lurton, T., Luyssaert, S., Madec, G., Madeleine, J., Maignan, F., Marchand, M., Marti, O., Mellul, L., Meurdesoif, Y., Mignot, J., Musat, I., Ottlé, C., Peylin, P., Planton, Y., Polcher, J., Rio, C., Rochetin, N., Rousset, C., Sepulchre, P., Sima, A., Swingedouw, D., Thiéblemont, R., Traore, A. K., Vancoppenolle, M., Vial, J., Vialard, J., Viovy, N., and Vuichard, N.: Presentation and Evaluation of the IPSL-CM6A-LR Climate Model, *Journal of Advances in Modeling Earth Systems*, 12, e2019MS002010, <https://doi.org/10.1029/2019MS002010>, 2020.

Chemke, R. and Coumou, D.: Human influence on the recent weakening of storm tracks in boreal summer, *npj Climate and Atmospheric Science*, 7, 86, <https://doi.org/10.1038/s41612-024-00640-2>, publisher: Nature Publishing Group, 2024.

Cherchi, A., Fogli, P. G., Lovato, T., Peano, D., Iovino, D., Gualdi, S., Masina, S., Scoccimarro, E., Materia, S., Bellucci, A., and Navarra, A.: Global Mean Climate and Main Patterns of Variability in the CMCC-CM2 Coupled Model, *Journal of Advances in Modeling Earth Systems*, 11, 185–209, <https://doi.org/10.1029/2018MS001369>, *\_eprint*: <https://agupubs.onlinelibrary.wiley.com/doi/pdf/10.1029/2018MS001369>, 2019.

D'Andrea, F., Duvel, J., Rivière, G., Vautard, R., Cassou, C., Cattiaux, J., Coumou, D., Faranda, D., Happé, T., Jézéquel, A., Ribes, A., and Yiou, P.: Summer Deep Depressions Increase Over the Eastern North Atlantic, *Geophysical Research Letters*, 51, e2023GL104435, <https://doi.org/10.1029/2023GL104435>, 2024.

Ding, Q. and Wang, B.: Circumglobal Teleconnection in the Northern Hemisphere Summer, *Journal of Climate*, 18, 3483–3505, <https://doi.org/10.1175/JCLI3473.1>, publisher: American Meteorological Society Section: *Journal of Climate*, 2005.

Donat, M. G., King, A. D., Overpeck, J. T., Alexander, L. V., Durre, I., and Karoly, D. J.: Extraordinary heat during the 1930s US Dust Bowl and associated large-scale conditions, *Climate Dynamics*, 46, 413–426, <https://doi.org/10.1007/s00382-015-2590-5>, 2016.

Dong, B., Sutton, R. T., Shaffrey, L., and Harvey, B.: Recent decadal weakening of the summer Eurasian westerly jet attributable to anthropogenic aerosol emissions, *Nature Communications*, 13, 1148, <https://doi.org/10.1038/s41467-022-28816-5>, publisher: Nature Publishing Group, 2022.

Eyring, V., Bony, S., Meehl, G. A., Senior, C. A., Stevens, B., Stouffer, R. J., and Taylor, K. E.: Overview of the Coupled Model Intercomparison Project Phase 6 (CMIP6) experimental design and organization, *Geoscientific Model Development*, 9, 1937–1958, <https://doi.org/10.5194/gmd-9-1937-2016>, publisher: Copernicus GmbH, 2016.

Fereday, D. and Knight, J.: The roles of atmospheric circulation and sea surface temperature in UK surface climate, *Atmospheric Science Letters*, 24, e1139, <https://doi.org/10.1002/asl.1139>, *\_eprint*: <https://rmets.onlinelibrary.wiley.com/doi/pdf/10.1002/asl.1139>, 2023.



Fiedler, S., van Noije, T., Smith, C. J., Boucher, O., Dufresne, J.-L., Kirkevåg, A., Olivié, D., Pinto, R., Reerink, T., Sima, A., and Schulz, M.: Historical Changes and Reasons for Model Differences in Anthropogenic Aerosol Forcing in CMIP6, *Geophysical Research Letters*, 50, e2023GL104848, <https://doi.org/10.1029/2023GL104848>, [\\_eprint: https://onlinelibrary.wiley.com/doi/pdf/10.1029/2023GL104848](https://doi.org/10.1029/2023GL104848), 2023.

Golaz, J.-C., Van Roekel, L. P., Zheng, X., Roberts, A. F., Wolfe, J. D., Lin, W., Bradley, A. M., Tang, Q., Maltrud, M. E., Forsyth, R. M., Zhang, C., Zhou, T., Zhang, K., Zender, C. S., Wu, M., Wang, H., Turner, A. K., Singh, B., Richter, J. H., Qin, Y., Petersen, M. R., Mamatjanov, A., Ma, P.-L., Larson, V. E., Krishna, J., Keen, N. D., Jeffery, N., Hunke, E. C., Hannah, W. M., Guba, O., Griffin, B. M., Feng, Y., Engwirda, D., Di Vittorio, A. V., Dang, C., Conlon, L. M., Chen, C.-C.-J., Brunke, M. A., Bisht, G., Benedict, J. J., Asay-Davis, X. S., Zhang, Y., Zhang, M., Zeng, X., Xie, S., Wolfram, P. J., Vo, T., Veneziani, M., Tesfa, T. K., Sreepathi, S., Salinger, A. G., Reeves Eyre, J. E. J., Prather, M. J., Mahajan, S., Li, Q., Jones, P. W., Jacob, R. L., Huebler, G. W., Huang, X., Hillman, B. R., Harrop, B. E., Foucar, J. G., Fang, Y., Comeau, D. S., Caldwell, P. M., Bartoletti, T., Balaguru, K., Taylor, M. A., McCoy, R. B., Leung, L. R., and Bader, D. C.: The DOE E3SM Model Version 2: Overview of the Physical Model and Initial Model Evaluation, *Journal of Advances in Modeling Earth Systems*, 14, e2022MS003156, [https://doi.org/https://doi.org/10.1029/2022MS003156](https://doi.org/10.1029/2022MS003156), e2022MS003156 2022MS003156, 2022.

335 Goldenberg, S. B., Landsea, C. W., Mestas-Nuñez, A. M., and Gray, W. M.: The Recent Increase in Atlantic Hurricane Activity: Causes and Implications, *Science*, 293, 474–479, <https://doi.org/10.1126/science.1060040>, publisher: American Association for the Advancement of Science, 2001.

Gutjahr, O., Putrasahan, D., Lohmann, K., Jungclaus, J. H., von Storch, J.-S., Brüggemann, N., Haak, H., and Stössel, A.: Max Planck 340 Institute Earth System Model (MPI-ESM1.2) for the High-Resolution Model Intercomparison Project (HighResMIP), *Geoscientific Model Development*, 12, 3241–3281, <https://doi.org/10.5194/gmd-12-3241-2019>, publisher: Copernicus GmbH, 2019.

Hanna, E., Fettweis, X., and Hall, R. J.: Brief communication: Recent changes in summer Greenland blocking captured by none of the 345 CMIP5 models, *The Cryosphere*, 12, 3287–3292, <https://doi.org/10.5194/tc-12-3287-2018>, 2018.

Happé, T., Van Straaten, C., Hamed, R., D'Andrea, F., and Coumou, D.: Observed circulation trends in boreal summer linked to two spatially 350 distinct teleconnection patterns, <https://doi.org/10.5194/egusphere-egu25-15844>, 2025.

Henley, B. J., Gergis, J., Karoly, D. J., Power, S., Kennedy, J., and Folland, C. K.: A Tripole Index for the Interdecadal Pacific Oscillation, *Climate Dynamics*, 45, 3077–3090, <https://doi.org/10.1007/s00382-015-2525-1>, 2015.

Hersbach, H., Bell, B., Berrisford, P., Hirahara, S., Horányi, A., Muñoz-Sabater, J., Nicolas, J., Peubey, C., Radu, R., Schepers, D., Sim- 355 mons, A., Soci, C., Abdalla, S., Abellán, X., Balsamo, G., Bechtold, P., Biavati, G., Bidlot, J., Bonavita, M., De Chiara, G., Dahlgren, P., Dee, D., Diamantakis, M., Dragani, R., Flemming, J., Forbes, R., Fuentes, M., Geer, A., Haimberger, L., Healy, S., Hogan, R. J., Hólm, E., Janisková, M., Keeley, S., Laloyaux, P., Lopez, P., Lupu, C., Radnoti, G., de Rosnay, P., Rozum, I., Vamborg, F., Vil- laume, S., and Thépaut, J.-N.: The ERA5 global reanalysis, *Quarterly Journal of the Royal Meteorological Society*, 146, 1999–2049, <https://doi.org/10.1002/qj.3803>, [\\_eprint: https://rmets.onlinelibrary.wiley.com/doi/pdf/10.1002/qj.3803](https://doi.org/10.1002/qj.3803), 2020.

Hoesly, R. M., Smith, S. J., Feng, L., Klimont, Z., Janssens-Maenhout, G., Pitkanen, T., Seibert, J. J., Vu, L., Andres, R. J., Bolt, R. M., Bond, 360 T. C., Dawidowski, L., Kholod, N., Kurokawa, J.-i., Li, M., Liu, L., Lu, Z., Moura, M. C. P., O'Rourke, P. R., and Zhang, Q.: Historical (1750–2014) anthropogenic emissions of reactive gases and aerosols from the Community Emissions Data System (CEDS), *Geoscientific Model Development*, 11, 369–408, <https://doi.org/10.5194/gmd-11-369-2018>, publisher: Copernicus GmbH, 2018.

Horton, D. E., Johnson, N. C., Singh, D., Swain, D. L., Rajaratnam, B., and Diffenbaugh, N. S.: Contribution of changes in atmospheric 365 circulation patterns to extreme temperature trends, *Nature*, 522, 465–469, <https://doi.org/10.1038/nature14550>, 2015.



370 Intergovernmental Panel On Climate Change (Ipcc): Climate Change 2021 – The Physical Science Basis: Working Group I Contribution to the Sixth Assessment Report of the Intergovernmental Panel on Climate Change, Cambridge University Press, 1 edn., ISBN 978-1-009-15789-6, <https://doi.org/10.1017/9781009157896>, 2023.

375 Kanamitsu, M., Ebisuzaki, W., Woollen, J., Yang, S.-K., Hnilo, J. J., Fiorino, M., and Potter, G. L.: NCEP–DOE AMIP-II Reanalysis (R-2), *Bulletin of the American Meteorological Society*, 83, 1631–1644, <https://doi.org/10.1175/BAMS-83-11-1631>, publisher: American Meteorological Society Section: *Bulletin of the American Meteorological Society*, 2002.

Kang, J. M., Shaw, T. A., and Sun, L.: Anthropogenic Aerosols Have Significantly Weakened the Regional Summertime Circulation in the Northern Hemisphere During the Satellite Era, *AGU Advances*, 5, e2024AV001318, <https://doi.org/10.1029/2024AV001318>, *\_eprint*: <https://onlinelibrary.wiley.com/doi/pdf/10.1029/2024AV001318>, 2024.

380 Kelley, M., Schmidt, G. A., Nazarenko, L. S., Bauer, S. E., Ruedy, R., Russell, G. L., Ackerman, A. S., Aleinov, I., Bauer, M., Bleck, R., Canuto, V., Cesana, G., Cheng, Y., Clune, T. L., Cook, B. I., Cruz, C. A., Del Genio, A. D., Elsaesser, G. S., Faluvegi, G., Kiang, N. Y., Kim, D., Lacis, A. A., Leboissetier, A., LeGrande, A. N., Lo, K. K., Marshall, J., Matthews, E. E., McDermid, S., Mezuman, K., Miller, R. L., Murray, L. T., Oinas, V., Orbe, C., García-Pando, C. P., Perlitz, J. P., Puma, M. J., Rind, D., Romanou, A., Shin-dell, D. T., Sun, S., Tausnev, N., Tsigaridis, K., Tselioudis, G., Weng, E., Wu, J., and Yao, M.-S.: GISS-E2.1: Configurations and Climatology, *Journal of Advances in Modeling Earth Systems*, 12, e2019MS002025, <https://doi.org/10.1029/2019MS002025>, *\_eprint*: <https://agupubs.onlinelibrary.wiley.com/doi/pdf/10.1029/2019MS002025>, 2020.

385 Knutti, R. and Sedláček, J.: Robustness and uncertainties in the new CMIP5 climate model projections, *Nature Climate Change*, 3, 369–373, <https://doi.org/10.1038/nclimate1716>, publisher: Nature Publishing Group, 2013.

390 Kosaka, Y., Kobayashi, S., Harada, Y., Kobayashi, C., Naoe, H., Yoshimoto, K., Harada, M., Goto, N., Chiba, J., Miyaoka, K., Sekiguchi, R., Deushi, M., Kamahori, H., Nakagawa, T., Tanaka, T. Y., Tokuhiro, T., Sato, Y., Matsushita, Y., and Onogi, K.: The JRA-3Q Reanalysis, . 2, 102, 49–109, <https://doi.org/10.2151/jmsj.2024-004>, 2024.

Lawrence, B. N., Bennett, V. L., Churchill, J., Juckles, M., Kershaw, P., Pascoe, S., Pepler, S., Pritchard, M., and Stephens, A.: Storing and manipulating environmental big data with JASMIN, in: 2013 IEEE International Conference on Big Data, pp. 68–75, <https://doi.org/10.1109/BigData.2013.6691556>, 2013.

395 Lewis, S. C., King, A. D., and Perkins-Kirkpatrick, S. E.: Defining a New Normal for Extremes in a Warming World, *Bulletin of the American Meteorological Society*, 98, 1139–1151, <https://doi.org/10.1175/BAMS-D-16-0183.1>, 2017.

Maddison, J. W., Catto, J. L., Hanna, E., Luu, L. N., and Screen, J. A.: Missing Increase in Summer Greenland Blocking in Climate Models, *Geophysical Research Letters*, 51, e2024GL108505, <https://doi.org/10.1029/2024GL108505>, 2024.

Robinson, A., Lehmann, J., Barriopedro, D., Rahmstorf, S., and Coumou, D.: Increasing heat and rainfall extremes now far outside the historical climate, *npj Climate and Atmospheric Science*, 4, 45, <https://doi.org/10.1038/s41612-021-00202-w>, 2021.

400 Rousi, E., Kornhuber, K., Beobide-Arsuaga, G., Luo, F., and Coumou, D.: Accelerated western European heatwave trends linked to more-persistent double jets over Eurasia, *Nature Communications*, 13, 3851, <https://doi.org/10.1038/s41467-022-31432-y>, 2022.

Scaife, A. A. and Smith, D.: A signal-to-noise paradox in climate science, *npj Climate and Atmospheric Science*, 1, 28, <https://doi.org/10.1038/s41612-018-0038-4>, publisher: Nature Publishing Group, 2018.

Schubert, S. D., Suarez, M. J., Pegion, P. J., Koster, R. D., and Bacmeister, J. T.: On the Cause of the 1930s Dust Bowl, *Science*, 303, 405 1855–1859, <https://doi.org/10.1126/science.1095048>, publisher: American Association for the Advancement of Science, 2004.

Seland, , Bentsen, M., Olivié, D., Toniazzo, T., Gjermundsen, A., Graff, L. S., Debernard, J. B., Gupta, A. K., He, Y.-C., Kirkevåg, A., Schwinger, J., Tjiputra, J., Aas, K. S., Bethke, I., Fan, Y., Griesfeller, J., Grini, A., Guo, C., Ilicak, M., Karsel, I. H. H., Landgren,



O., Liakka, J., Moseid, K. O., Nummelin, A., Spensberger, C., Tang, H., Zhang, Z., Heinze, C., Iversen, T., and Schulz, M.: Overview of the Norwegian Earth System Model (NorESM2) and key climate response of CMIP6 DECK, historical, and scenario simulations, 410 *Geoscientific Model Development*, 13, 6165–6200, <https://doi.org/10.5194/gmd-13-6165-2020>, 2020.

Shepherd, T. G.: Atmospheric circulation as a source of uncertainty in climate change projections, *Nature Geoscience*, 7, 703–708, 415 <https://doi.org/10.1038/ngeo2253>, publisher: Nature Publishing Group, 2014.

Smith, D. M., Gillett, N. P., Simpson, I. R., Athanasiadis, P. J., Baehr, J., Bethke, I., Bilge, T. A., Bonnet, R., Boucher, O., Findell, K. L., 420 Gastineau, G., Gualdi, S., Hermanson, L., Leung, L. R., Mignot, J., Müller, W. A., Osprey, S., Otterå, O. H., Persad, G. G., Scaife, A. A., Schmidt, G. A., Shiogama, H., Sutton, R. T., Swingedouw, D., Yang, S., Zhou, T., and Ziehn, T.: Attribution of multi-annual to decadal changes in the climate system: The Large Ensemble Single Forcing Model Intercomparison Project (LESFMIP), *Frontiers in Climate*, 4, 425 <https://doi.org/10.3389/fclim.2022.955414>, publisher: Frontiers, 2022.

Smith, D. M., Dunstone, N. J., Eade, R., Hardiman, S. C., Hermanson, L., Scaife, A. A., and Seabrook, M.: Mitigation needed to avoid unprecedeted multi-decadal North Atlantic Oscillation magnitude, *Nature Climate Change*, 15, 403–410, <https://doi.org/10.1038/s41558-025-02277-2>, 2025.

Swart, N. C., Cole, J. N. S., Kharin, V. V., Lazare, M., Scinocca, J. F., Gillett, N. P., Anstey, J., Arora, V., Christian, J. R., Hanna, S., Jiao, Y., Lee, W. G., Majaess, F., Saenko, O. A., Seiler, C., Seinen, C., Shao, A., Sigmond, M., Solheim, L., von Salzen, K., Yang, D., and Winter, B.: The Canadian Earth System Model version 5 (CanESM5.0.3), *Geoscientific Model Development*, 12, 4823–4873, 430 <https://doi.org/10.5194/gmd-12-4823-2019>, 2019.

Tang, S., Qiao, S., Wang, B., Liu, F., Zhu, X., Feng, T., Feng, G., and Dong, W.: Recent changes in ENSO's impacts on the summertime circumglobal teleconnection and mid-latitude extremes, *Nature Communications*, 16, 646, <https://doi.org/10.1038/s41467-025-55925-8>, publisher: Nature Publishing Group, 2025.

Tatebe, H., Ogura, T., Nitta, T., Komuro, Y., Ogochi, K., Takemura, T., Sudo, K., Sekiguchi, M., Abe, M., Saito, F., Chikira, M., Watanabe, S., Mori, M., Hirota, N., Kawatani, Y., Mochizuki, T., Yoshimura, K., Takata, K., O'ishi, R., Yamazaki, D., Suzuki, T., Kurogi, M., Kataoka, 435 T., Watanabe, M., and Kimoto, M.: Description and basic evaluation of simulated mean state, internal variability, and climate sensitivity in MIROC6, *Geoscientific Model Development*, 12, 2727–2765, <https://doi.org/10.5194/gmd-12-2727-2019>, publisher: Copernicus GmbH, 2019.

Teng, H., Leung, R., Branstator, G., Lu, J., and Ding, Q.: Warming Pattern over the Northern Hemisphere Midlatitudes in Boreal Summer 1979–2020, *Journal of Climate*, 35, 3479–3494, <https://doi.org/10.1175/JCLI-D-21-0437.1>, publisher: American Meteorological Society Section: *Journal of Climate*, 2022.

Trenberth, K. E. and Shea, D. J.: Atlantic hurricanes and natural variability in 2005, *Geophysical Research Letters*, 33, 440 <https://doi.org/10.1029/2006GL026894>, \_eprint: <https://agupubs.onlinelibrary.wiley.com/doi/pdf/10.1029/2006GL026894>, 2006.

Vautard, R., Cattiaux, J., Happé, T., Singh, J., Bonnet, R., Cassou, C., Coumou, D., D'Andrea, F., Faranda, D., Fischer, E., Ribes, A., Sippel, S., and Yiou, P.: Heat extremes in Western Europe increasing faster than simulated due to atmospheric circulation trends, *Nature Communications*, 14, 6803, <https://doi.org/10.1038/s41467-023-42143-3>, 2023.

Wilks, D. S.: Statistical methods in the atmospheric sciences, vol. 100 of *International geophysics series*, Academic press, third edn., ISBN 978-0-12-385022-5, 2011.

Yukimoto, S., Koshiro, T., Kawai, H., Oshima, N., Yoshida, K., Urakawa, S., Tsujino, H., Deushi, M., Tanaka, T., Hosaka, M., Yoshimura, H., Shindo, E., Mizuta, R., Ishii, M., Obata, A., and Adachi, Y.: MRI MRI-ESM2.0 model output prepared for CMIP6 CMIP, [https://www.wdc-climate.de/ui/entry?acronym=C6\\_5243961](https://www.wdc-climate.de/ui/entry?acronym=C6_5243961), 2023.



Zhang, K., Zuo, Z., Mei, W., Zhang, R., and Dai, A.: A westward shift of heatwave hotspots caused by warming-enhanced land–air coupling, *Nature Climate Change*, 15, 546–553, <https://doi.org/10.1038/s41558-025-02302-4>, publisher: Nature Publishing Group, 2025.

Ziehn, T., Chamberlain, M. A., Law, R. M., Lenton, A., Bodman, R. W., Dix, M., Stevens, L., Wang, Y.-P., and Srbinsky, J.: The Australian Earth System Model: ACCESS-ESM1.5, *Journal of Southern Hemisphere Earth Systems Science*, 70, 193–214,

450 <https://doi.org/10.1071/ES19035>, 2020.